

somebody make a fancy title page

1 Introduction

somebody write an introduction

bl.a. mention

- where we get the forward model from and what it does (this will not be explained in the following section)
- that we need the forward model to do the inverse model (which was the actual task)

2 Validation of the Forward Model

The forward model computes from a set of oceanic and atmospheric parameters the brightness temperatures expected to be measured by a satellite radiometer. The input parameters are listed in Table 1, and the output parameters include values for both horizontal and vertical polarization at 6.93 GHz, 10.65 GHz, 18.70 GHz, 23.80 GHz, and 36.50 GHz.

| | Forward Model | | Reference Data | |
|-------------------------|---------------|---------------|----------------|-------------------|
| | Abbrev. | Unit | Abbrev. | Unit |
| Ice concentration | C_is | fraction | ci | fraction |
| MY-fraction | F_MY | fraction | | |
| Ice temperature | T_is | K | skt | K |
| Water vapour | V | mm (columnar) | tcwv | kg/m ² |
| Cloud liquid water | L | mm (columnar) | tclw | kg/m ² |
| Wind speed | W | m/s | ws | m/s |
| Sea surface temperature | T_ow | K | sst | K |

Table 1: Atmospheric and oceanic parameters entered into the forward model

This forward model was validated by comparing its results to reference data from ESA’s “Sea Ice Climate Change Initiative”.

2.1 Description of the Reference Data

The reference data consists of brightness temperatures at the relevant polarizations and frequencies as measured by the AMSR2 radiometer onboard the GCOM-W1 satellite. The measured data is paired with validated sea ice concentrations and numerical weather predictions for the atmospheric and oceanic parameters at the same geocoded locations at near simultaneous time. There are two different data sets: one with an ice concentration of 0, the other one with an ice concentration of 1. The data points of each set cover the entire year 2014. The dataset with the no ice condition covers latitudes between 5 and 73 degrees, and the dataset with an ice concentration of 1 covers latitudes between 78.5 and 87.5 degrees. A description of the dataset can be found in [2].

2.1.1 Potential Sources of Errors

When using this reference data package to validate the forward model, several points have to be taken into account: Firstly, the forward model was developed for the AMSR-E instrument. To use the atmospheric and oceanic parameters as input in the forward model in order to compare the output with the AMSR2 measured brightness temperatures, we applied a conversion to these brightness temperatures as suggested in [5].

Secondly, the reference data does not contain information about the multi-year ice fraction needed as input in the forward model. For the data set with an ice concentration of 0, the MY fraction is irrelevant. It is therefore possible to validate the forward model for the open water datapoints. For the data set with an ice concentration of 1, a multi-year ice concentration of 0.5 was assumed. This dataset can therefore be used as a coherency check, but not to validate the model. The

sensitivity of the brightness temperatures computed by the forward model to a variation in the multi-year ice fraction is discussed in ??.

Thirdly, as mentioned above, the geophysical parameters given in the reference data were computed from numerical weather predictions, and their uncertainty is not known. In particular, this is also not discussed in [2]. We suspect the error on the cloud liquid water to be especially large. This parameter is increasingly influential towards higher frequency channels, were an error in the prediction would accordingly cause a larger error in the brightness temperatures.

2.1.2 Practical Considerations

The wind speed is given in the reference data as a u-component, v-component, and as a composite of the two. We chose to use the composite value for the wind speed as the input in the forward model. The parameters “water vapour” and “cloud liquid water”, which are given in the columnar units of kg/m^2 in the reference data, were converted to mm, indicating the height of water vapor or cloud liquid water if condensed uniformly across the column. 1 kg/m^2 corresponds to 1 mm [3].

2.2 Validation Procedure

For the data set with an ice concentration of 0, the atmospheric and oceanic parameters were entered into the forward model, and the difference between the modelled brightness temperatures and the corrected brightness temperatures from the reference data was recorded:

$$e = T_{\text{B, modelled}} - T_{\text{B, reference, corrected}}$$

The reference file has 6988 data points, every second of which was used. For the data set with an ice concentration of 1, the atmospheric and oceanic parameters were entered together with guessed values for the multi-year ice fraction of 0, 0.5, and 1, consecutively. The multi-year ice fraction was chosen to be constant for all datapoints to simplify the validation process. Of the 10936 reference data points recorded between October and May, every second point was used.

2.3 Validation Results

The discrepancies for the no ice condition are shown in Table 2, and those for the ice condition are shown in Tables 3 to 5.

| Channel | 6.93v | 6.93h | 10.65v | 10.65h | 18.70v | 18.70h |
|-----------|----------|-----------|-----------|-----------|-----------|-----------|
| Mean | 0.1027 K | −0.2817 K | −1.1832 K | −2.8420 K | 3.7785 K | 1.8898 K |
| Std. Dev. | 1.4176 K | 2.9155 K | 2.1227 K | 3.7947 K | 10.2530 K | 12.9650 K |

| Channel | 23.80v | 23.80h | 36.50v | 36.50h |
|-----------|-----------|-----------|-----------|-----------|
| Mean | −1.5822 K | −4.7026 K | −2.2742 K | −5.8099 K |
| Std. Dev. | 3.6383 K | 7.1321 K | 4.6630 K | 10.2386 K |

Table 2: Modelled brightness temperatures compared to the corrected no-ice dataset

In addition, histograms were plotted for the error distribution of the no ice condition (only for the channels with the most notable offset), as well as of the ice condition for a multi-year ice

concentration of 0.5 (all channels). These are shown in Figures 1 and 2. The occurrence rate is normalized to the number of data points. It can be observed, that the channels for 10.65 GHz and higher frequencies have double peaks, which could correspond to the points of no/full ice concentration in the data set. All channels have a negative bias, i.e. the modelled brightness temperatures are smaller than the ones in the reference data.

| Channel | 6.93v | 6.93h | 10.65v | 10.65h | 18.70v | 18.70h |
|-----------|------------|------------|------------|------------|-----------|------------|
| Mean | −18.8904 K | −36.1881 K | −18.8032 K | −30.2216 K | −4.7582 K | −11.3865 K |
| Std. Dev. | 4.9079 K | 7.4777 K | 5.6295 K | 9.6398 K | 11.0927 K | 14.1847 K |

| Channel | 23.80v | 23.80h | 36.50v | 36.50h |
|-----------|-----------|-----------|-----------|-----------|
| Mean | 1.3569 K | −1.4115 K | 9.5846 K | 9.5860 K |
| Std. Dev. | 14.3928 K | 16.7768 K | 19.4340 K | 20.2949 K |

Table 3: Modelled brightness temperatures compared to the corrected dataset with an ice concentration of 1, multi-year ice fraction 0

| Channel | 6.93v | 6.93h | 10.65v | 10.65h | 18.70v | 18.70h |
|-----------|------------|------------|------------|------------|------------|------------|
| Mean | −13.0277 K | −22.3905 K | −16.9252 K | −22.8343 K | −10.8922 K | −15.9716 K |
| Std. Dev. | 5.0466 K | 7.5811 K | 5.6564 K | 9.6501 K | 11.0802 K | 14.1971 K |

| Channel | 23.80v | 23.80h | 36.50v | 36.50h |
|-----------|-----------|-----------|-----------|-----------|
| Mean | −7.9716 K | −8.9957 K | −6.1945 K | −4.2009 K |
| Std. Dev. | 14.4112 K | 16.8180 K | 19.4457 K | 20.3167 K |

Table 4: Modelled brightness temperatures compared to the corrected dataset with an ice concentration of 1, multi-year ice fraction 0.5

| Channel | 6.93v | 6.93h | 10.65v | 10.65h | 18.70v | 18.70h |
|-----------|-----------|-----------|------------|------------|------------|------------|
| Mean | −7.1651 K | −8.5928 K | −15.0473 K | −15.4471 K | −17.0261 K | −20.5568 K |
| Std. Dev. | 5.1993 K | 7.7493 K | 5.6848 K | 9.6754 K | 11.0758 K | 14.2130 K |

| Channel | 23.80v | 23.80h | 36.50v | 36.50h |
|-----------|------------|------------|------------|------------|
| Mean | −17.3001 K | −16.5760 K | −21.9737 K | −17.9878 K |
| Std. Dev. | 14.4461 K | 16.8686 K | 19.4906 K | 20.3633 K |

Table 5: Modelled brightness temperatures compared to the corrected dataset with an ice concentration of 1, multi-year ice fraction 1

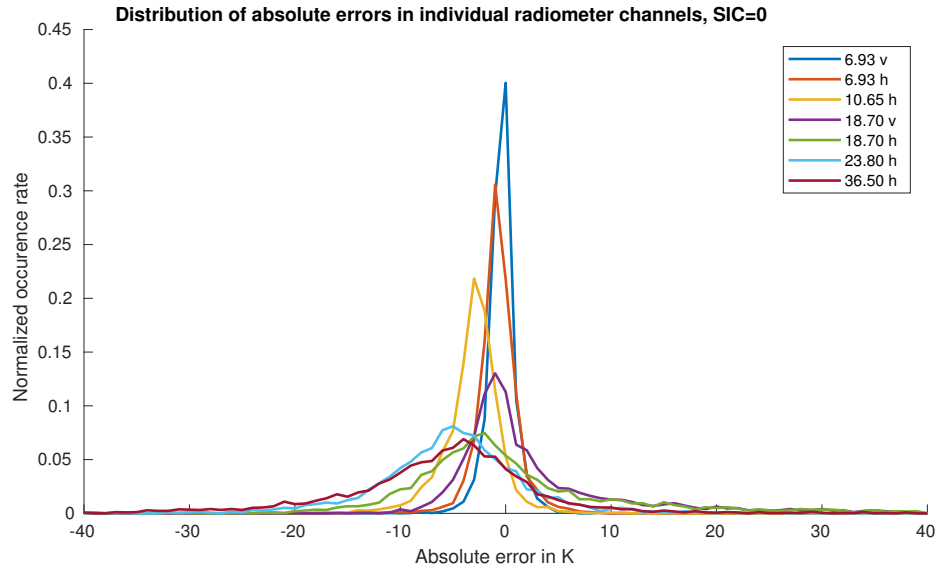


Figure 1: Distribution of the errors of the modelled brightness temperatures compared to the no ice dataset; only some channels are shown

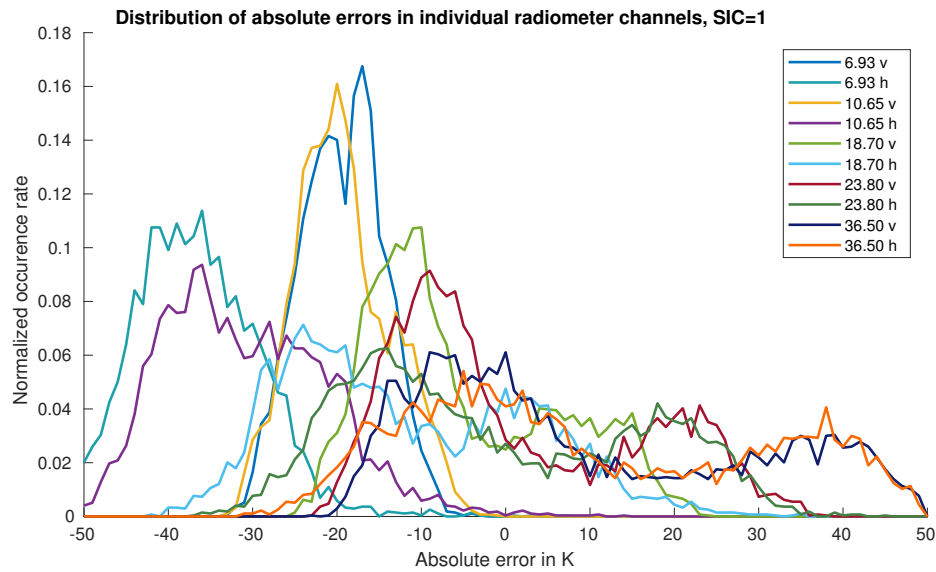


Figure 2: Distribution of the errors of the modelled brightness temperatures compared to the no ice dataset; multi-year ice concentration 0.5

The forward model is not under all conditions able to reproduce the brightness temperatures expected from the reference data. We do not know, which of the contributions listed in section 2.1.1 causes the errors. To further investigate this problem is beyond the scope of this project, and we will therefore limit our use of the model to no ice cases for the following tasks.

3 Development of the Inverse Model

To compute the oceanic and atmospheric parameters from the set of brightness temperatures measured by the satellite radiometer, an inverse model was developed using estimation theory. The inverse model essentially employs the forward model to compute an estimate of the brightness temperatures from an estimate of the geophysical parameters, then compares the estimated brightness temperatures to the measured brightness temperatures, and finally improves the estimate for the geophysical parameters based on the result of the comparison (see figure 3 for a graphical representation). Once the estimated brightness temperatures come close enough to the measured ones, the geophysical parameters last inputted are considered a good estimate and delivered as the result of the inverse modelling. This is explained in more detail in the next subsection.

The inverse model was then validated by comparing it to the forward model. It was not compared to any external data source.

3.1 Algorithm of the Inverse Model

The input of the inverse model function is a 10 element vector $T_{B,m}$ containing the brightness temperatures measured for each of the radiometer channels.

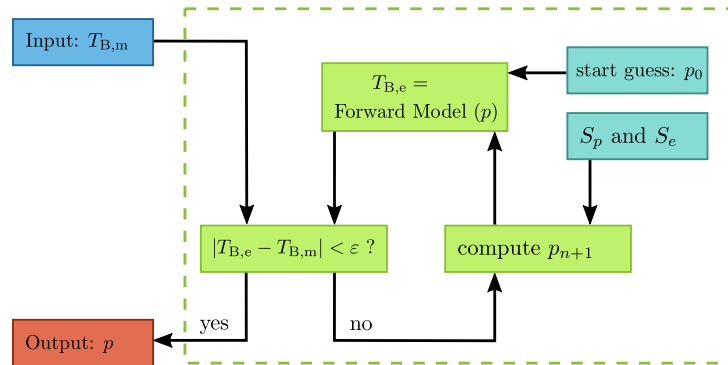


Figure 3: Blockdiagram of the inverse model function

The inverse model enters a 7 element vector p containing estimates of the geophysical parameters listed in table 1 into the forward model and retrieves a 10 element vector $T_{B,e}$ containing estimated brightness temperatures for each channel. In the first iteration, p is a generic guess, which is hard coded into the inverse model function. The estimated brightness temperatures $T_{B,e}$ are then compared to the measured brightness temperatures $T_{B,m}$.

If the estimated and the measured brightness temperatures do not agree within a range of ε , a vector p_{n+1} for the $(n+1)^{\text{th}}$ iteration is computed from the vector p_n of the current iteration as follows:

$$p_{n+1} = p_n + \left(S_p^{-1} + M_n^T S_e^{-1} M_n \right)^{-1} \cdot \left(M_n^T S_e^{-1} (T_{B,m} - T_{B,e,n}) + S_p^{-1} (p_0 - p_n) \right)$$

Herein, S_p is the 7 by 7 covariance matrix of the geophysical parameters indicating the uncertainty attached to the start guess. Small values on the diagonal of this matrix correspond to a high confidence in the start guess and cause p_{n+1} to be close to p_0 . S_e is the 10 by 10 covariance

matrix of the brightness temperatures measured by the radiometer. Small values on the diagonal of this matrix correspond to a high confidence into the accuracy of the radiometer, and much weight is assigned to the difference between the estimated and measured brightness temperatures, accordingly.

M_n is a 7 by 10 matrix, and it contains the partial derivatives of the brightness temperatures with respect to the geophysical parameters. This matrix is computed for every iteration. To find the element in the i^{th} line and j^{th} column of M , the i^{th} geophysical parameter is perturbed slightly, the forward model is called for the altered vector p , and the resulting perturbation of the brightness temperature in the j^{th} channel is recorded. The partial derivative is then obtained by dividing the brightness temperature perturbation by the perturbation of the geophysical parameter. Large values in M correspond to a high sensitivity of the radiometer to changes in the geophysical parameters.

The partial derivatives are only valid for those values of p at which they were computed - i.e. those of the past iteration. The inverse model extrapolates these derivatives to find p_{n+1} for the next iteration. If the relations of the geophysical parameters and the brightness temperatures were entirely linear, this extrapolation would be entirely accurate and only one iteration would be needed to find the suitable vector p . The less linear the system is, the less accurate is the extrapolation, and the more iterations are needed.

If the estimated and the measured brightness temperatures do agree within a range of ε , the current vector p is outputted as a sufficiently accurate estimation of the geophysical parameters.

3.2 Choice of Model Parameters

Suitable values for the start guess of the atmospheric and oceanic parameters (p_0) and for the covariance matrix S_p were found by computing the mean and variance of the individual parameters from the reference data sets. As the data sets cover all seasons and almost the entire globe (see section 2.1.1), we believe this reference to be a broad enough base for computing a generic mean and variance. The values for both are listed below; the elements being in the order wind speed, water vapour, liquid water, sea surface temperature, ice temperature, ice concentration, multiyear ice fraction. The units correspond to those given in table 1.

$$p_0 = \begin{pmatrix} 6.1327 & 7.7035 & 0.0295 & 273.5503 & 265.0088 & 0.5000 & 0.5000 \end{pmatrix}$$

$$S_p = \begin{pmatrix} 9.2865 & 0 & 0 & 0 & 0 & 0 & 0 \\ 0 & 62.1415 & 0 & 0 & 0 & 0 & 0 \\ 0 & 0 & 0.0056 & 0 & 0 & 0 & 0 \\ 0 & 0 & 0 & 22.5386 & 0 & 0 & 0 \\ 0 & 0 & 0 & 0 & 98.6461 & 0 & 0 \\ 0 & 0 & 0 & 0 & 0 & 1 & 0 \\ 0 & 0 & 0 & 0 & 0 & 0 & 1 \end{pmatrix}$$

For each of the radiometer channels, an uncertainty of 0.4 K was assumed. This leads to 0.16 K² for each element of the diagonal of S_e .

3.3 Validation of Inverse Model

The inverse model is intended to be an inversion of the forward model. This means that in comparison to any reference, the inverse model can at most be as accurate as the forward model. The inverse model was therefore validated by comparison to the forward model:

- for a given set of geophysical parameters, brightness temperatures were computed by the forward model
- these brightness temperatures were entered into the inverse model, which computed an estimate of the geophysical parameters ($p_{\text{estimated}}$)
- the estimate was then compared to the original set of geophysical parameters (p_{original}), the error being described as follows:

$$e = p_{\text{estimated}} - p_{\text{original}}$$

The reference data sets used to validate the forward model were used as a generic source of geophysical parameters to be inputted into the forward model. They were not used as a reference to compare modelled results to! Unfortunately, the data sets contain some outliers, which cause the inverse model to not converge. We therefore restricted the number of iterations to 10 to be able to automatically run the inversion model on all data points. The results of the inverse model did not improve for a higher number of iterations.

Using all data points of the no ice data file, the inverse model produces the error described in Table 6. A closer investigation revealed that the error does not arise evenly distributed over the used input data points: for high sea surface temperatures, which come together with high amounts of liquid and gaseous water in the atmosphere, the error can become very large. This is exemplarily illustrated in Figure 4, where the input sea surface temperature (p_{original}) is shown together with the error on the sea surface temperature (e) produced by the inverse model.

| Parameter | ws [m/s] | tcwv [kg/m ²] | tclw [kg/m ²] | sst [K] | ci [fraction] |
|-----------|----------|---------------------------|---------------------------|---------|---------------|
| Mean | -0.3915 | 0.0927 | 0.0013 | -1.2479 | 0.0236 |
| Std. Dev. | 6.4720 | 5.5608 | 0.0798 | 16.6951 | 0.4234 |

Table 6: Estimated parameters compared to the original parameters

When the input data is restricted to points with a sea surface temperature below 283 K, the accuracy of the inverse model improves. This excludes 2492 data points. The remaining error is described in Table 7.

| Parameter | ws [m/s] | tcwv [kg/m ²] | tclw [kg/m ²] | sst [K] | ci [fraction] |
|-----------|----------|---------------------------|---------------------------|---------|---------------|
| Mean | -0.5640 | 0.0216 | 0.0011 | -0.5747 | 0.0065 |
| Std. Dev. | 1.0443 | 0.0499 | 0.0066 | 0.5919 | 0.0131 |

Table 7: Estimated parameters compared to the original parameters, with the input data restricted to points with a sea surface temperature below 283 K

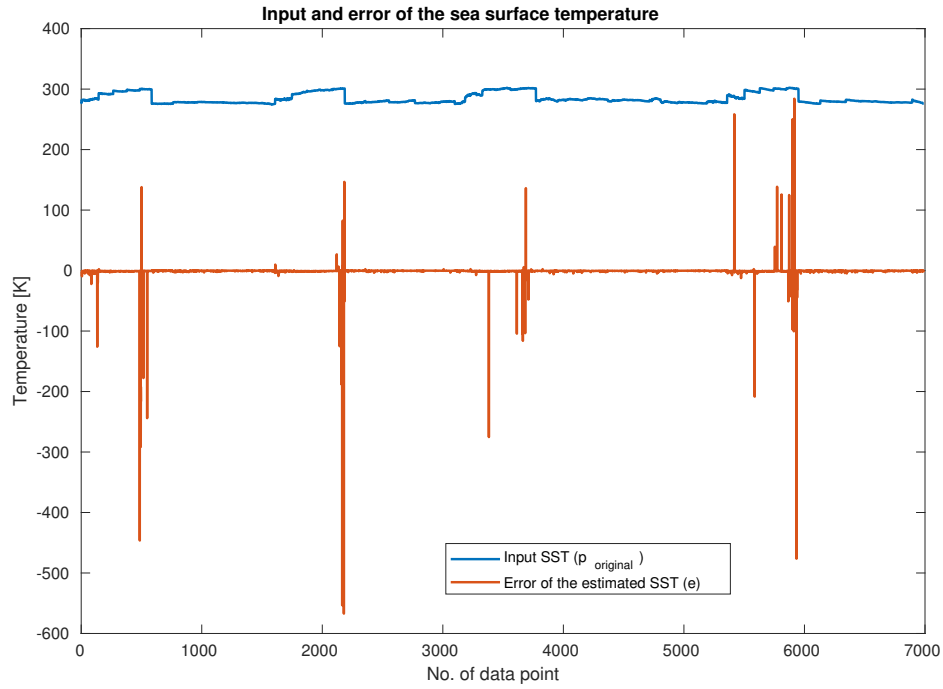


Figure 4: The error of the inverse model (red) can become very large for high sea surface temperatures (blue).

We conclude that the inverse model is very sensible to high sea surface temperatures and atmospheric water contents, but performs satisfactory otherwise.

References

- [1] Dorte Hofman-Bang, Forward algorithm, September 2003.
http://www.seaice.dk/exercises/task3/Matlab/FW_funktion2_is.m
[accessed: 18/11/2017]
- [2] Round Robin Data Package Manual, Version 2.0/, July 2017. Ref: SICCI SIC RRDP-07-17.
http://www.seaice.dk/undervisning/Sotiris/SICCI_RRDB_Manual_v2.01_20170717.docx [accessed: 18/11/2017]
- [3] (unit conversion) <http://www.remss.com/measurements/atmospheric-water-vapor/> [accessed: 18/11/2017]
- [4] C. Elachi, Introduction to the Physics and Techniques of Remote Sensing. John Wiley and Sons, 1987. (section 6.5+7.3)
- [5] Kyle. A. Hilburn and Chelle L. Gentemann, AMSR2 Calibration: Intercomparison of RSS and JAXA Brightness Temperatures, unpublished.